Published in *IET Syst. Biol.* **2**, 48-54 (2008).

Phase Coupling in the Cardiorespiratory Interaction

A. Bahraminasab,* D. Kenwright, A. Stefanovska, F. Ghasemi, P. V. E. McClintock†

Abstract

Markovian analysis is applied to derive nonlinear stochastic equations for the reconstruction of heart rate and respiration rate variability data. A model of their *phase* interactions is obtained for the first time, thereby gaining new insights into the strength and direction of the cardiorespiratory phase coupling. The reconstructed model can reproduce synchronization phenomena between the cardiac and respiratory systems, including switches in synchronization ratio. The technique is equally applicable to the extraction of the multi-dimensional couplings between many interacting subsystems.

1 Introduction

Biological oscillators are found at every level of complexity, and for almost every living system [1]. Oscillations arise through the interaction of many dynamical degrees of freedom and processes with different time scales [2]. Oscillatory signals from the human cardiovascular system (CVS) have been analysed over several decades because they appear to contain so much clinically relevant information. For diagnostic purposes, however, it seems still to be the case that only classical time-series analysis methods are being applied [3]. As each new technique of time-series analysis has emerged with the development of nonlinear and stochastic dynamics, it was challenged by application to CVS data and, in particular, to the analysis of cardio-respiratory interactions. Heart rate variability (HRV) has attracted particular attention, whereas respiratory rate variability (RRV) has been less studied. Several additional oscillatory processes were also shown to be involved in cardiovascular interactions, e.g. the myogenic, neurogenic, and endothelial-related metabolic activities [4]. The underlying dynamics is complex, nonlinear, time-varying, and subject to fluctuations [5, 6, 7], so that no single time-series analysis method can be expected to reveal all relevant properties. It must therefore be insufficient for diagnosis of many pathological states.

Because of the complexity, a parametric model of the cardiovascular system is essential. Once it has been constructed, its parameters (e.g. amplitudes, phases and coupling coefficients) could characterise the *state* of the subject and thus be used both for earlier diagnosis of CVS disease and for assessing the efficacy of treatment. Cardio-respiratory interactions have been modelled from first principles (see [8] and references therein). Yet, because the system is so complex and present physiological knowledge is still insufficient [9], this group of models is of limited utility and often not realistic. Moreover, it was mainly amplitude dynamics that was considered. Because time-series data are now easily measured and widely available, the inverse approach based on recorded data seems more promising. However, very few techniques are available for modelling nonlinear and stochastic dynamics. The recently introduced Bayesian inference technique [10, 11], or a Markov approach [12], may provide the solution to this as yet unsolved problem. The inference technique has already been applied to the *amplitude* dynamics of the cardio-respiratory interaction, whereas

*Corresponding author.

†A. Bahraminasab,a.bahraminasab@lancaster.ac.uk, D. Kenwright, A. Stefanovska and, P. V. E. McClintock are with the Department of Physics, Lancaster University, Lancaster, LA1 4YB, UK. F. Ghasemi is with the Max-Planck-Institut für Physik komplexer Systeme, Nöthnitzer Strasse 38, D 01187 Dresden, Germany.

the Markov approach has not yet been applied to the problem. Coupled oscillators interact both through their amplitudes and phases. There is a crucial distinction between phase and amplitude investigations in that small perturbations have a huge impact on the phase, but only a very small effect on the amplitude. Analysis of phase dynamics has recently been used to reveal synchronization properties [13, 14, 15], nonlinearities [16], and the directionality of the inter-oscillator interactions [17, 18, 19]. Both HRV and RRV have so far been used only in synchronization or directionality analysis and no known modelling attempts have been made to date.

The heart is the main pump in the CVS. The latter consists of a large network of vessels that can be regarded as resistances or conductances. The ultimate goal of the circulation is to supply all cells with O_2 and nutrients. So optimal control of the amount of blood, and thus of O_2 and nutrients, is needed. This is performed by controlling the cardiac frequency and the stroke volume, the amount of blood expelled by the heart in each cycle. The cardiac frequency and stroke volume adapt to variations in the conductance of the vascular network. In addition, the conductances are regulated by local mechanisms such as the endothelial, neurogenic and myogenic activities. The other generator in the network is the respiratory system, which not only takes care of the O_2 but also modulates the heart rate and stroke volume. The respiratory modulation of the heart rate has long been known as respiratory sinus arrythmia (RSA) [20, 21], while the other mechanisms are presently the subject of intensive research [7, 22, 23, 24].

In fact it is cardiac *output*, the product of heart rate and stroke volume, that is regulated. While the stroke volume is rather constant, the heart rate varies to take account of the needs of the body. It is also well known that the respiratory frequency changes significantly when the system is perturbed, e.g. during anæsthesia [25], or in diabetes [24]. Frequency dynamics is therefore a powerful, objective and noninvasive tool to explore the dynamics of the system and can in principle improve our understanding of the physiology and the health of a subject.

In this paper we apply the theory of multidimensional Markovian processes to cardio-respiratory data for the first time, analyse HRV and RRV data simultaneously, and model cardio-respiratory *phase* interactions. Mathematical modelling of system dynamics is combined with the extraction of model parameters directly from measured time series. We analyzed recordings of cardiac and respiratory activity from healthy volunteers in repose using, respectively, a 3-lead ECG system and piezoresistive sensor attached to a belt around the thorax. The measurements were non-invasive and of length 30 minutes (10 subjects) or 80 minutes (8 subjects). The instantaneous frequencies of the cardiac and respiratory oscillations (HRV and RRV) were extracted using the marked events method [26]. For the first time, we reconstruct a model by simultaneous consideration of the phase dynamics of the cardiac and respiratory oscillations.

2 The mathematics of Markov processes

The theory of multidimensional Markovian processes [27] was applied to the data as follows. Consider the two-dimensional stochastic variable

$$\mathbf{q}(t) = \begin{pmatrix} \tilde{f}_h(t) \\ \tilde{f}_r(t) \end{pmatrix}, \tag{1}$$

where $\tilde{f}_i(t) = \frac{f_i(t)-\bar{f}_i}{\sigma_i}$, $i = h, r$, f_h and f_r are the instantaneous heart (HRV) and respiratory (RRV) frequencies, $\bar{f}_h$ and $\bar{f}_r$ are their averages, and σ_h and σ_r are the HRV and RRV variances. The stochastic process underlying the evolution of $\mathbf{q}$ during the time t is Markovian if the conditional probability density function (pdf) $P\left(\mathbf{q}(t_1)|\mathbf{q}(t_2), \mathbf{q}(t_3), ..., \mathbf{q}(t_N)\right)$ with $t_N \leq t_{N-1} \leq ... \leq t_1$ for a *certain* time interval $t_M = t_2 - t_1$, fulfills the relation $P(\,\mathbf{q}(t_1)\,|\,\mathbf{q}(t_2), \mathbf{q}(t_3), ..., \mathbf{q}(t_N)\,) = P(\,\mathbf{q}(t_1)\,|\,\mathbf{q}(t_2)\,)$. For Markov processes,

the evolution of the conditional pdf can be described by the Kramers-Moyal expansion which, by Pawula's theorem, truncates after the second term if the fourth order expansion coefficient vanishes. In this case, the Kramers-Moyal expansion reduces to a Fokker-Planck equation [27]. Alternatively, the stochastic process underlying the evolution of $\mathbf{q}$ can be described by the Langevin equation for $\mathbf{q}(t)$:

$$\frac{\partial}{\partial t} q_i(t) \;=\; f_i(\mathbf{q},t) \;+\; \sum_{j=1}^{2} g_{ij}(\mathbf{q},t)\Gamma_j(t)\;. \tag{2}$$

The components of $\mathbf{\Gamma}(t)$ represent the stochastic influences acting on the process. In this case, the functions $\mathbf{f}(\mathbf{q},t)$ and $\mathbf{g}(\mathbf{q},t)$ can be calculated from the drift vector $\mathbf{D}^{(1)}$ and the diffusion matrix $\mathbf{D}^{(2)}$. In Stratanovich's stochastic calculus, $\mathbf{f}(\mathbf{q},t)$ and $\mathbf{g}(\mathbf{q},t)$ are given by

$$\begin{aligned} f_i(\mathbf{q},t) &= D_i^{(1)}(\mathbf{q},t) - (\sqrt{\mathbf{D}^{(2)}})_{kj}\frac{\partial}{\partial q_k}(\sqrt{\mathbf{D}^{(2)}})_{ij}, \\ g_{ij}(\mathbf{q},t) &= (\sqrt{\mathbf{D}^{(2)}})_{ij}, \end{aligned} \tag{3}$$

where the drift vector $\mathbf{D}^{(1)}$ and the diffusion matrix $\mathbf{D}^{(2)}$ are defined as

$$\begin{aligned} D_i^{(1)}(\mathbf{q},t) &= \lim_{t_M\to 0}\frac{1}{t_M}\langle (q_i'(t-t_M)-q_i(t))\,|\,\mathbf{q},t\rangle, \\ D_{ij}^{(2)}(\mathbf{q},t) &= \lim_{t_M\to 0}\frac{1}{2t_M}\langle (q_i'(t-t_M)-q_i(t))\times \\ &\qquad (q_j'(t-t_M)-q_j(t))|\mathbf{q},t\rangle. \end{aligned} \tag{4}$$

Here $\langle\cdot\rangle$ are conditional expectation values that can easily be determined from experimental data. Moreover, $\sqrt{\mathbf{D}^{(2)}}$ is to be calculated by diagonalizing the matrix $\mathbf{D}^{(2)}$, taking the square root of each element of the diagonalized matrix and transforming the result back into the original system of coordinates. We have used a data analysis technique that yields estimates for drift and diffusion functions of Markov diffusion processes [28]. Accordingly, drift and diffusion functions are given in terms of truncated function series with expansion parameters computed from experimental data. Note that the conditional averages D^1 and D^2 are not necessarily continuously differentiable functions with respect to t. Therefore, it is important to note that the derivatives correspond to derivatives from above. In this case, we have used a procedure which is discussed in detail in a paper by Frank et. al [28]. Accordingly, the phase space is decomposed into bins. This decomposition of the phase space into bins suggests that we may usefully decompose D^1 and D^2 in a similar way. After that, the drift and diffusion functions expressed as polynomials of $\bar{f}_i$. This step-wise decomposition of drift and diffusion coefficients has been successfully applied in a number of cases [29, 30, 31, 32, 33, 34]. We comment, however, that this step-wise decomposition introduces an inaccuracy of $\mathrm{O}(\Delta f_i, \Delta t)$ where Δf_i is the resolution of f_i and $1/\Delta t$ is sampling frequency[28]. The Langevin equation offers an alternative way of checking the Markovian properties of a stochastic variable. The idea [30] is to estimate the coefficients $\mathbf{D}^{(1)}$ and $\mathbf{D}^{(2)}$ from experimental data according to (4), and to calculate $\mathbf{f}$ and $\mathbf{g}$ using (3); the Langevin equation (2) can then be used to extract $\mathbf{\Gamma}(t)$ from the (measured) derivatives of the $q_i(t)$. If the realizations of the stochastic force obtained by this method are δ-correlated with zero mean and a Gaussian distribution, the Markov condition is fulfilled. We use this method here because, for multidimensional stochastic variables, it is hardly possible to check the Markov condition directly by means of multiconditional pdfs. Also the numerical cost for the estimation of the coefficients $\mathbf{D}^{(k)}$ of order three and higher grows considerably with the order k (growth $\propto 2^k$).

3 Inferred Model

We now apply the above method to the fluctuations in HRV and RRV. Using (4) directly, we calculate the drift and diffusion coefficients, $D_i^{(1)}$ and $D_{ij}^{(2)}$. We start with the HRV component of the drift vector. Using experimental data, it will be shown that the dependence of $D_h^{(1)}$ on $\tilde{f}_h$ can to a good approximation be described by a straight line, as $D_h^{(1)} = a + b\tilde{f}_h$. Although we have a first order dependence (with small scatter) for a with different values of $\tilde{f}_r$, the b-component of the drift vector shows a second-order dependence on the $\tilde{f}_r$ (Fig. 1). The second-order coefficient $D_{hh}^{(2)}$ is almost constant, for example in Fig. 2 $D_{hh}^{(2)}$ is shown as a function of $\tilde{f}_r$, which shows no clear functional dependence on $\tilde{f}_r$. Before we proceed with the $\tilde{f}_r$-components of the drift vector and diffusion matrix, note that $D_{hr}^{(2)}$ fluctuates approximately around zero (Fig. 2). We take this as evidence that the mixed coefficient $D_{hr}^{(2)}$ vanishes. Given that these off-diagonal elements vanish, the functions $\mathbf{g}(\tilde{f}_h, \tilde{f}_r)$ in (2) can easily be calculated according to equation (3) and $\mathbf{g}$ is then simply given by:

$$g_{hh} = \sqrt{D_{hh}^{(2)}}, \qquad g_{hr} = g_{rh} = 0, \qquad g_{rr} = \sqrt{D_{rr}^{(2)}}. \tag{5}$$

From the results obtained so far the Langevin-equation (2) for $\tilde{f}_r$ takes the form:

$$\frac{\partial}{\partial t}\tilde{f}_h(t) \quad = \quad D_h^{(1)}(\tilde{f}_h, \tilde{f}_r) + \sqrt{D_{hh}^{(2)}}\,\Gamma_h(t). \tag{6}$$

It can already be used to extract the h–component $\Gamma_h(t)$ of the stochastic force from measured realizations of $\frac{\partial}{\partial t}\tilde{f}_h(t)$, $\tilde{f}_h$, and $\tilde{f}_r(t)$. The stochastic process governing the t–evolution of the stochastic variable $\mathbf{q}(t)$ is Markovian, if the stochastic force $\mathbf{\Gamma}$ is δ–correlated. As can be seen in Fig. 3, the correlation function of the stochastic force $\Gamma_h(t)$ fluctuates around zero, clearly indicating that the Markovian properties are fulfilled, in agreement with [35] which for healthy subjects the Markov length scale is less than 5 steps. To complete the description by Markov analysis, we still have to determine the coefficients $D_r^{(1)}$ and $D_{rr}^{(2)}$. $D_r^{(1)}$ turns out to be a linear function of the $\tilde{f}_r$ and does not depend explicitly on $\tilde{f}_h$, and the coefficient $D_{rr}^{(2)}$ turns out to be a second order function of just $\tilde{f}_r$. Hence

$$\begin{aligned} D_r^{(1)}(\tilde{f}_r, \tilde{f}_h) &= D_r^{(1)}(\tilde{f}_r) = a' + b'\tilde{f}_r \\ D_{rr}^{(2)}(\tilde{f}_r, \tilde{f}_h) &= D_{rr}^{(2)}(\tilde{f}_r) = c + d\tilde{f}_r + e\tilde{f}_r^2, \end{aligned} \tag{7}$$

and for $\tilde{f}_r$ the Langevin-equation (2) takes the form:

$$\frac{\partial}{\partial t}\tilde{f}_r(t) = D_r^{(1)}(\tilde{f}_r) - \frac{d}{d\tilde{f}_r}(D_{rr}^{(2)}(\tilde{f}_r)) + \sqrt{D_{rr}^{(2)}(\tilde{f}_r)}\Gamma_r(t). \tag{8}$$

For other data measured from different subjects, we expect the functional dependence of drift coefficients and diffusion matrices to be the same, but with different numerical coefficients (cf. Table 1). The dynamics of $D_h^{(1)}$ and $D_{hh}^{(2)}$ is as shown in Fig. 4, and the average values can be seen to be close to those in Table. 1 obtained from the whole signals. The functionality of the coefficients obtained indicates that the frequency of respiration influences the cardiac frequency strongly, whereas the influence is very small in the opposite direction, consistent with the results of methods specifically developed for detecting the coupling directionality of interacting phases [18, 19], and with direct physiological observations.

Table 1 shows that the values of the drift and diffusion coefficients vary considerably from one subject to another. One possible explanation is that we have a wide range of ages (from 22 to 72 yr) and that the drift and diffusion coefficients are age-dependent. Moreover, although, we have divided all the signals by their variances, there is still a large inter-subject variability which is probably attributable

Subject	$D_h^{(1)}(\tilde{f}_h, \tilde{f}_r)$	$D_{hh}^{(2)}(\tilde{f}_h, \tilde{f}_r)$
1	0.16-0.01$\tilde{f}_r$-(0.32-0.04$\tilde{f}_r$+0.69$\tilde{f}_r^2$)$\tilde{f}_h$	0.15
2	-0.06-0.09$\tilde{f}_r$-(0.39-0.01$\tilde{f}_r$+0.27$\tilde{f}_r^2$)$\tilde{f}_h$	0.21
3	-0.04+0.01$\tilde{f}_r$-(0.27-0.19$\tilde{f}_r$+0.25$\tilde{f}_r^2$)$\tilde{f}_h$	0.16-0.04$\tilde{f}_r$
4	0.01 -0.03$\tilde{f}_r$-(0.06-0.02$\tilde{f}_r$+0.09$\tilde{f}_r^2$)$\tilde{f}_h$	0.02
5	-0.01 -0.03$\tilde{f}_r$-(0.20-0.12$\tilde{f}_r$+0.17$\tilde{f}_r^2$)$\tilde{f}_h$	0.15

Subject	$D_r^{(1)}(\tilde{f}_r)$	$D_{rr}^{(2)}(\tilde{f}_r)$
1	-0.02-0.74$\tilde{f}_r$	0.09+0.06$\tilde{f}_r$+0.43$\tilde{f}_r^2$
2	-0.01-0.45$\tilde{f}_r$	0.21+0.05$\tilde{f}_r$+0.17$\tilde{f}_r^2$
3	-0.10-0.71$\tilde{f}_r$	0.28+0.37$\tilde{f}_r$+0.46$\tilde{f}_r^2$
4	-0.05 -0.71$\tilde{f}_r$	0.27+0.12$\tilde{f}_r$+0.36$\tilde{f}_r^2$
5	-0.05-0.82$\tilde{f}_r$	0.18-0.05$\tilde{f}_r$+0.47$\tilde{f}_r^2$

Table 1: The drift coefficients and diagonal components of the diffusion Matrix for 5 out of 18 subjects (the first 3 are 30 minute and the rest are 80 minute).

to from the differing natures and histories of the subjects. Nevertheless, for all subjects the drift and diffusion coefficients for respiration, as well as the diffusion coefficients for heart, do not vary by very much. The situation is more complicated in the case of the drift coefficient of the heart. This may suggest that the heart interacts with many more sources of variability than just with respiration.

4 Validation - synchronization analysis

We now have two equations related to HRV and RRV. To check the accuracy of estimation we have analyzed and compared the synchronization behavior of the original and reconstructed pairs of signals. The results are shown in Fig. 5 and 6. In Fig. 5 the reconstructed signals related to HRV and RRV have been plotted versus the original (labelled as "Real" in the figures) signals.

Classically, synchronization of two periodic nonidentical oscillators is understood as an adjustment of their rhythms, or locking of their phases, $\phi_{n,m} = n\phi_1 - m\phi_2 = \text{const}$, where ϕ_1 and ϕ_2 are phases, n and m are integers, and $\phi_{n,m}$ is the generalized phase difference, or relative phase. For noisy, chaotic systems and/or systems with modulated natural frequencies a weaker condition of phase synchronization, $|\phi_{n,m}| = |n\phi_1 - m\phi_2 - \delta| < \text{const}$, where δ is some (average) phase shift, was introduced [36, 37, 38, 39]. Accordingly, synchronization is then understood as the appearance of peaks in the distribution of cyclic relative phase $\psi_{n,m} = \phi_{n,m} \mod 2\pi$ and interpreted as the existence of a preferred stable value of phase difference between two oscillators. In such a case, the n:m phase locking is manifested as a time variation of $\psi_{n,m}$ around a horizontal plateau.

In analyzing synchronization, the integers n and m should both be determined. In the case of two interacting noisy oscillatory processes, n and m change in time. One possibility, known as the phase stroboscope, or synchrogram, is to fix the value of m and observe changes of n in time [40]. Accordingly, the cardiorespiratory synchrogram is constructed by plotting the normalized relative phase of a heartbeat within m respiratory cycles, $\Psi_m = \frac{1}{2\pi}(\phi_2(t_k) \mod 2\pi m)$, where t_k is the time of kth heartbeat and ϕ_2 is the instantaneous phase of respiration. We calculated the normalized relative phase, Ψ_m, directly from the measured data, exploiting the fact that both signals contain sharp peaks that clearly mark the instantaneous cycles. Each successive peak was marked as an equivalence of one oscillatory cycle, corresponding to which a 2π increment was added. The instantaneous phase is then

$$\phi(t) = 2\pi \frac{t - t_k}{t_k + 1 - t_k} + 2\pi k, \qquad t_k \le t < t_{k+1}, \tag{9}$$

where t_k is time of kth marker event. Defined in this way the phase is a monotonically increasing piecewise-linear function of time defined on the real line. Usually, the first step in searching an n:m locking is look for horizontal plateaus in Ψ_m, revealing the value of n in cases when synchronization exists. The distribution of $\Psi_{n,m}$ is then a δ function, smeared in the presence of noise. For strongly nonlinear oscillators it can be nonuniform even in the absence of noise [41]. To characterize the strength of synchronization we therefore need a robust quantitative measure. Since in noisy systems phase synchronization can be understood in a statistical sense as the existence of preferred values of the generalized phase difference, measures based on quantifying the distribution of phases

$$\eta = \phi_2 \mod 2\pi n|_{\phi_1 \mod 2\pi m} \tag{10}$$

were proposed. We will use an index based on conditional probability which was introduced in [39] and was shown to facilitate reliable detection of synchronous epochs of different order n:m [42]. Accordingly, the phase of the second oscillator is observed at fixed values of the phase of the first oscillator, θ. The interval of each phase ϕ_1 and ϕ_2, $[0, 2\pi m)$ and $[0, 2\pi n)$, respectively, is divided into N bins. The values of $\phi_1 \mod 2\pi m$ that belong to bin l are denoted as θ_l , while the number of points inside this bin is denoted as M_l , and, by using Eq. (10), M_l values of $\eta_{j,l}, j = 1, ..., M_l$, are calculated. If there is no synchronization between the oscillators, a uniform distribution of $\eta_{j,l}$ can be expected on the interval $[0, 2\pi n)$, or else it clusters around a certain value resulting in a unimodal distribution. Hence, the distribution is quantified as

$$r_l(t_k) = \frac{1}{M_l} \sum_{j=1}^{M_l(t_k)} e^{i\phi_2(t_j)} \tag{11}$$

for each j when $\phi_1(t_j)$ belongs to the lth bin and $t_k - t_p/2 \leq t_j < tk + t_p/2$. $M_l(t_k)$ is the number of points in this bin at the kth instant. An average over $\sim$8 periods, t_p, of the slower oscillator was used. Where the phases are completely locked, or completely unlocked we obtain $|r_l(t_k)| = 1$ or $|r_l(t_k)| = 0$, respectively. To improve reliability, we also calculate the average over all bins and obtain the index of synchronization $\lambda_{n,m}(t_k) = \frac{1}{N} \sum_{l=1}^{N} |r_l(t_k)|$.

Accordingly, $\lambda_{n,m}$ is a measure of the conditional probability that ϕ_2 has a certain value within the lth bin when ϕ_1 belongs to this bin. Synchronization can occur in several regimes, switching from one index to another with time. The indices used must be found by trial and error, although a good indication of where the regimes occur can be obtained from the frequency ratio of the two oscillators. A frequency ratio of $\frac{f_1}{f_2} = 4$ would suggest m:n indices of 1:4. As we mentioned before, perfect synchronization appears when the value of the index = 1, and is zero when there is no synchronization. However, in a noisy system such as the CVS, perfect synchronization is rarely seen. Hence a high index value close to 1 is used as an indication of synchronization. For the present investigation, values above 0.9 were taken to validate evidence of possible synchronization seen in the synchrograms.

Also, there is the problem of apparent synchronization that occurs by pure coincidence. As a test, shuffled data was created from pairs of HRV and RRV signals, as well as from the reconstructed ones: in the shuffling process, these data were randomized in such a way that no real synchronization could exist. It was found that short epochs above the threshold did indeed occur occasionally, but that they lasted no more than $\sim$25 seconds in length, as illustrated in Figs. 6(B)and (D). Hence, only epochs exceeding 25 seconds were considered as representing true synchronization. Using these two criteria it was possible to give a picture of likely synchronization regimes. The synchronization indices show that, instead of there being long episodes of n:m synchronization with constant n and m, the cardiorespiratory interaction switches in time between several close ratios. This switching could either be representative of the onset of chaos or just an indication that there are other oscillatory components on slower time scales that perturb the pattern of synchronization almost periodically.

Fig. 6 shows that these results demonstrate convincingly that the nonlinear Langevin equations derived from experimental data provide a valid description of cardiorespiratory dynamics. These results reveal another important aspect of applying a Markov approach to the cardiorespiratory interaction. Fig. 6 illustrates transitions between the 2:11 and 1:5 synchronization states. They are thought to arise from interactions between the different oscillatory components in the cardiorespiratory signals. Fig. 6 shows the correctness of this idea. Synchronization episodes derived from two Langevin equations show almost the same transitions between synchronization states. The small differences between the original and reconstructed graph may be related to the effect of other oscillatory components, e.g. the myogenic, neurogenic, or endothelial-related metabolic activities [7], which have not been considered here. **We also comment that, to make a prediction for the future of the signal we could select a few (say 3) consecutive points in the experimental series and search for the three consecutive points in the reconstructed series, derived from Langevin equations, that differ least from the selected points. Note that the better the estimations of drift and diffusion and the longer the time series (better statistics), the better and more complete the reconstruction that can be expected. If the process were** *exactly* **Markovian then we could use these Langevin equations to predict any quantity involved in the problem. In reality, of course, all of the discussion relates to Markovianicity within some range of accuracy.**

5 Discussion and conclusion

Like the Bayesian inference method [10], the Markovian approach can in principle be applied to any signals, including multi-dimensional ones arising from complex interactions between many subsystems. The two methods differ radically, however, in that the former is an analytical extension of the generalized least squares method, whereas the latter is based on the analytical information of the Markov processes. The method proposed here is in some ways similar to that discussed in the paper by Frank et all [28] which describes model identification from trajectory measurements in nonlinear stochastic equation with state-dependent (multiplicative) white noise. The drift $h(x)$ and diffusion $D(x)$ coefficients as functions of a state variable x ($D_i^{(1)}(f_h, f_r)$ and $D_{ij}^{(2)}(f_h, f_r)$ in the present paper) are obtained using definitions following from the Fokker Planck equation, i.e. as conditional averages involving first and second moments of the system trajectory displacement from the point x during an infinitesimal time interval. The method presented in the paper by Frank et al gives asymptotically correct values for $h(x)$ and $D(x)$ in the limit of an infinitely large number of measurements, but it may not provide a very accurate statistical analysis of the problem for a limited .

Where the number of observations is relatively small, certain regions of the state variable x (corresponding to the tails of the probability distribution of x in the dynamical problem) may contain only a few data points. In such cases, discretization with a constant bin size is not the optimal approach. Correct analysis requires one to choose a bin size adaptively for different regions of x, depending on the particular observations, with wider bins where there are fewer dat points. Alternatively, it is possible to completely avoid binning of the configuration space by introduction of a posterior distribution of model parameters conditioned on the measured trajectory points. This approach, introduced in a recent paper by Smelyanskiy et al [10], is based on a path integral representation of the stochastic process and a functional series expansion of the empirically chosen basis functions in the dynamical model. As mentioned above this approach avoids binning of the measured trajectory points and computes directly a posterior distribution of the unknown model parameters with computational complexity equal to that in Frank et al. On the other hand, it may not always be easy to guess *a priori* which type of the model and how many different basis functions will be appropriate. Nevertheless, with suitable initial, inference method should gives accurate results even for short time series.

In summary, the model reconstructed by the Markovian approach reproduces the coupling directionality, strength, and phase dynamics of the cardiac and respiratory oscillations and their interactions. **The fundamental time scale in the approach is the Markov time scale, which is the minimum time interval over which the series can be considered as constituting a Markov process. Based on the estimates of the Kramers- Moyal coefficients for the series, it was shown that the fourth-order coefficient is very small, implying that the Kramers-Moyal expansion reduces to a Fokker-Planck equation which, in turn, is equivalent to a Langevin equation. Thus, the probability densities of the fluctuations satisfy a Fokker-Planck equation. It is characterized by drift and diffusion coefficients, representing the first two coefficients in the Kramers-Moyal expansion. We computed accurate approximants for the coefficients of the stochastic time series by using the polynomial ansatz. We then constructed two simple Langevin equations governing the time series. The resulting equations are capable of providing a rational explanation for complex features of the series. Moreover, it requires no scaling feature. Our approach also reveals in detail the statistical properties of the data, which can help one to check the biological modelling rather precisely.**

6 Acknowledgment

The authors would like to thank V. N. Smelyanskiy for a very useful discussion. This work was supported by the Wellcome Trust and by the FP6 EU NEST-Pathfinder project “BRACCIA”.

References

[1] P. E. Rapp. Atlas of cellular oscillations. *J. Exp. Biol.*, 81:281–306, 1979.

[2] A. T. Winfree. *The Geometry of Biological Time*. Springer-Verlag, New York, 1980.

[3] A. J. Camm, M. Malik, J. T. Bigger, and *et al.* Heart rate variability – Standards of measurement, physiological interpretation, and clinical use. *Circulation*, 93(5):1043–1065, 1996.

[4] A. Stefanovska. *Self-Organisation of Biological Systems Influenced by Electric Currents*, PhD thesis. University of Ljubljana, Ljubljana, 1992.

[5] J. P. Saul, D. T. Kaplan, and R. I. Kitney. Nonlinear interactions between respiration and heart rate: classical physiology of entrained nonlinear oscillators. In K. L. Ripley, editor, *Computers in Cardiology*, pages 299–302. IEEE Comput. Soc. Press, Washington, 1989.

[6] K. H. Chon, T. J. Mullen, and R. J. Cohen. A dual-input nonlinear system analysis of autonomic modulation of heart rate. *IEEE Trans. Biomed. Eng.*, 43(5):530–544, 1996.

[7] A. Stefanovska and M. Bračič. Physics of the human cardiovascular system. *Contemporary Phys.*, 40(1):31–55, 1999.

[8] D. G. Luchinsky, M. M. Millonas, V. N. Smelyanskiy, A. Pershakova, A. Stefanovska, and P. V. E. McClintock. Nonlinear statistical modeling and model discovery for cardiorespiratory data. *Phys. Rev. E*, 72(2):021905, 2005.

[9] D. L. Eckberg. The human respiratory gate. *J. Physiol. (Lond.)*, 548(2):339–352, 2003.

[10] V. N. Smelyanskiy, D. G. Luchinsky, A. Stefanovska, and P. V. E. McClintock. Inference of a nonlinear stochastic model of the cardiorespiratory interaction. *Phys. Rev. Lett.*, 94(9):098101, 2005.

[11] W. Edwards, H. Lindman, and L. J. Savage. Bayesian statistical- inference for physiological research. *Psychological Review*, 70(3):193–242, 1963.

[12] H. Haken. *Synergetics, An Introduction*. Springer, Berlin, 1983.

[13] C. Schäfer, M. G. Rosenblum, J. Kurths, and H. H. Abel. Heartbeat synchronised with ventilation. *Nature*, 392(6673):239–240, 1998.

[14] M. B. Lotrič and A. Stefanovska. Synchronization and modulation in the human cardiorespiratory system. *Physica A*, 283(3-4):451–461, 2000.

[15] N. B. Janson, A. G. Balanov, V. S. Anishchenko, and P. V. E. McClintock. Phase synchronization between several interacting processes from univariate data. *Phys. Rev. Lett.*, 86(9):1749–1752, 2001.

[16] J. Jamšek, A. Stefanovska, and P. V. E. McClintock. Nonlinear cardio-respiratory interactions resolved by time-phase bispectral analysis. *Phys. Med. Biol.*, 49(18):4407–4425, 2004.

[17] T. Schreiber. Measuring information transfer. *Phys. Rev. Lett.*, 85(2):461–464, July 2000.

[18] M. G. Rosenblum, L. Cimponeriu, A. Bezerianos, A. Patzak, and R. Mrowka. Identification of coupling direction: Application to cardiorespiratory interaction. *Phys. Rev. E.*, 65(4):041909, 2002.

[19] M. Paluš and A. Stefanovska. Direction of coupling from phases of interacting oscillators: An information-theoretic approach. *Phys. Rev. E*, 67:055201(R), 2003.

[20] S. Hales. *Statistical Essays II, Hæmastatisticks*. Innings Manby, London, 1773.

[21] C. Ludwig. Beiträge zur Kenntniss des Einflusses der Respirationsbewegungen auf den Blatlauf im Aortensysteme. *Arch. Anat. Physiol. und Wiss. Med.*, 13:242–302, 1847.

[22] A. Stefanovska, M. Bračič, and H. D. Kvernmo. Wavelet analysis of oscillations in the peripheral blood circulation measured by laser Doppler technique. *IEEE Trans. Bio. Med. Eng.*, 46(10):1230–1239, 1999.

[23] P. Kvandal, S. A. Landsverk, A. Bernjak, U. Benko, A. Stefanovska, H. D. Kvernmo, and K. A. Kirkebøen. Low frequency oscillations of the laser Doppler perfusion signal in human skin. *Microvasc. Res.*, 2006.

[24] V. Urbančič-Rovan, B. Meglič, A. Stefanovska, A. Bernjak, K. Ažman-Juvan, and A. Kocijančič. Incipient cardiovascular autonomic imbalance revealed by wavelet analysis of heart rate variability in type 2 diabetic patients. (Diabetic Med., 24(1):18–26, 2007.

[25] B. Musizza, A. Stefanovska, P. V. E. McClintock, M. Paluš, J. Petrovčič, S. Ribarič, and F. F. Bajrović. Interactions between cardiac, respiratory, and EEG-δ oscillations in rats during anæsthesia. (J. Physiol. (London)), 580(1):315–326, 2007.

[26] M. Chavez, M. Besserve, C. Adam, and J. Martinerie. Towards a proper estimation of phase synchronization from time series. *J. Neurosc. Meth.*, 154(1-2):149–160, 2006.

[27] H. Risken. *The Fokker–Planck Equation*. Springer-Verlag, Berlin, 1984.

[28] T. D. Frank, M. Sondermann, T. Ackemann, and R. Friedrich. Parametric data analysis of bistable stochastic systems. *Nonlinear Phenomena in Complex Systems*, 8(2):193 – 199, 2005.

[29] R. Friedrich and J. Peinke. Description of a turbulent cascade by a Fokker-Planck equation. *Phys. Rev. Lett.*, 78(5):863–866, Feb 1997.

[30] S. Siegert, R. Friedrich, and J. Peinke. Analysis of data sets of stochastic systems. *Phys. Lett. A*, 243(5–6):275–280, 1998.

[31] R. Friedrich, J. Peinke, and Ch. Renner. How to quantify deterministic and random influences on the statistics of the foreign exchange market. *Phys. Rev. Lett.*, 84(22):5224–5227, May 2000.

[32] J. Gradišek, S. Siegert, R. Friedrich, and I. Grabec. Analysis of time series from stochastic processes. *Phys. Rev. E*, 62(3):3146–3155, Sep 2000.

[33] G. R. Jafari, S. M. Fazeli, F. Ghasemi, S. M. V. Allaei, M. R. R. Tabar, A. I. Zad, and G. Kavei. Stochastic analysis and regeneration of rough surfaces. *Phys. Rev. Lett.*, 91(22):226101, Nov 2003.

[34] H. U. Bödeker, M. C. Röttger, A. W. Liehr, T. D. Frank, R. Friedrich, and H.-G. Purwins. Noise-covered drift bifurcation of dissipative solitons in a planar gas-discharge system. *Phys. Rev. E*, 67(5):056220, May 2003.

[35] M. R. R. Tabor, F. Ghasemi, J. Peinke, R. Friedrich, K. Kaviani, F. Taghavi, S. Sadeghi, G. Bizhani, and M. Sahimi. New computational approaches to the analysis of interbeat intervals in human subjects. *Computing in Science and Engineering*, 8(2):54–65, 2006.

[36] M. G. Rosenblum, A. S. Pikovsky, and J. Kurths. Phase synchronization of chaotic oscillators. *Phys. Rev. Lett.*, 76(11):1804–1807, 1996.

[37] A. S. Pikovsky, M. G. Rosenblum, G. V. Osipov, and J. Kurths. Phase synchronization of chaotic oscillators by external driving. *Physica D*, 104(3-4):219–238, 1997.

[38] A. Pikovsky, M. Rosenblum, and J. Kurths. *Synchronization – A Universal Concept in Nonlinear Sciences*. Cambridge University Press, Cambridge, 2001.

[39] P. Tass, M. G. Rosenblum, J. Weule, J. Kurths, A. Pikovsky, J. Volkmann, A. Schnitzler, and H.-J. Freund. Detection of n:m phase locking from noisy data: Application to magnetoencephalography. *Phys. Rev. Lett.*, 81(15):3291–3294, 1998.

[40] M. G. Rosenblum, A. S. Pikovsky, J. Kurths, C. Schäfer, and P. Tass. Phase synchronization: From theory to data analysis. In F. Moss and S. Gielen, editors, *Handbook of Biological Physics*, volume 4, pages 279–321. Elsevier, Amsterdam, 2001.

[41] A. Stefanovska, H. Haken, P. V. E. McClintock, M. Hožič, F. Bajrović, and S. Ribarič. Reversible transitions between synchronization states of the cardiorespiratory system. *Phys. Rev. Lett.*, 85(22):4831–4834, 2000.

[42] A. Stefanovska. Cardiorespiratory interactions. *Nonlinear Phenomena in Complex Systems*, 5(4):462–469, 2002.

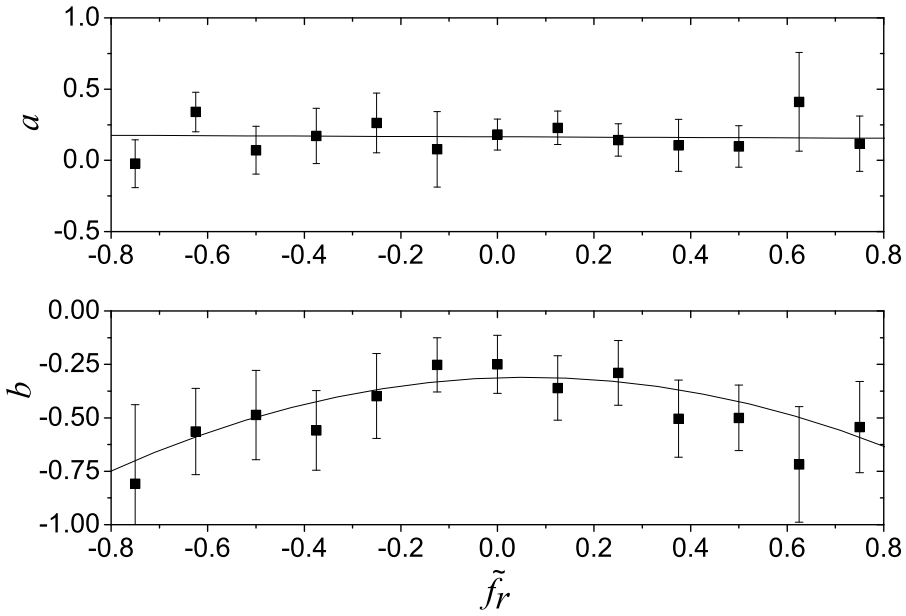

Figure 1: Plots of a and b as functions of $\tilde{f}_r$ in the drift coefficient of HRV, $D_h^{(1)} = a + b\tilde{f}_h$, derived from the HRV and RRV signals of Subject 1. The average and variance of their HRV were $\bar{f}_h = 1.21$ Hz and $\sigma_h = 0.18$ Hz respectively; for RRV, the average and variance were $\bar{f}_r = 0.237$ Hz and $\sigma_r = 0.025$ Hz.

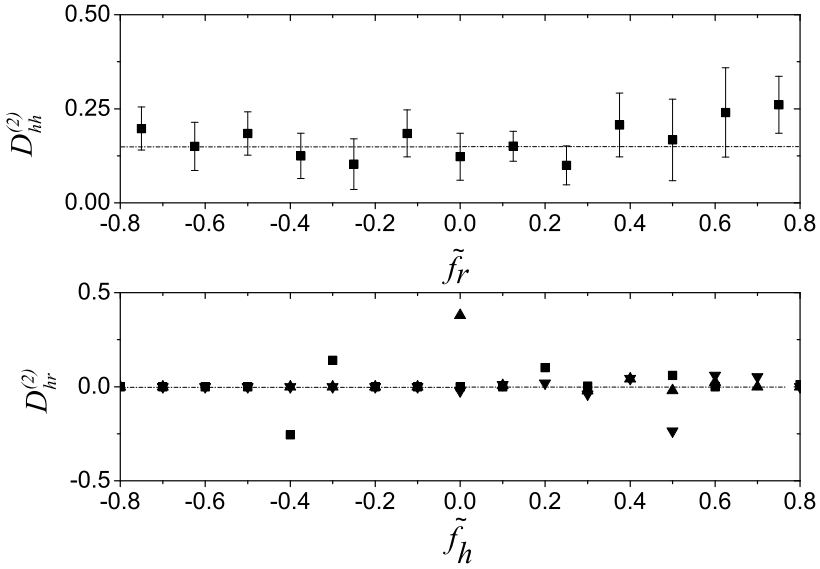

Figure 2: The hh-component $D_{hh}^{(2)}$ of the diffusion matrix (top) related to Subject 1 in the same domain of frequency of the drift coefficient. The hr-component $D_{hr}^{(2)}$ of the diffusion matrix (bottom) for Subject 1 as a function of $\tilde{f}_r$ for $\tilde{f}_r = -\sigma_r$ (gradient), $\tilde{f}_r = 0$ (squares) and $\tilde{f}_r = +\sigma_r$ (triangle). The coefficient $D_{hr}^{(2)}$ shows fluctuations around zero.

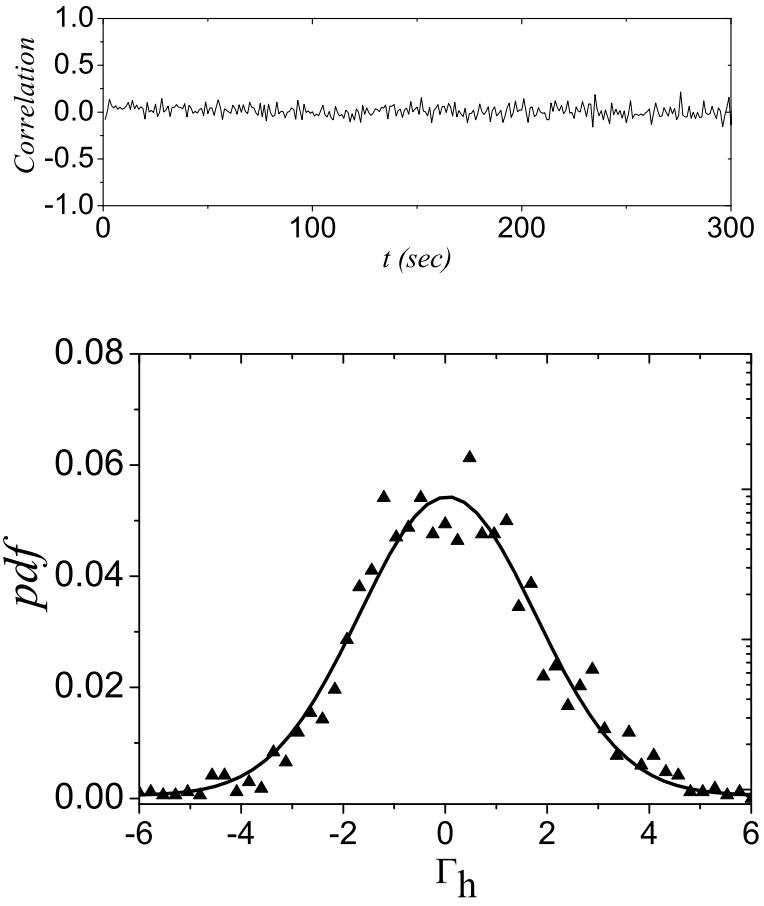

Figure 3: The correlation function of the $\tilde{f}_h$-component of the stochastic force $\mathbf{\Gamma}(t)$(top) and its pdf (bottom) fitted by a Gaussian function.

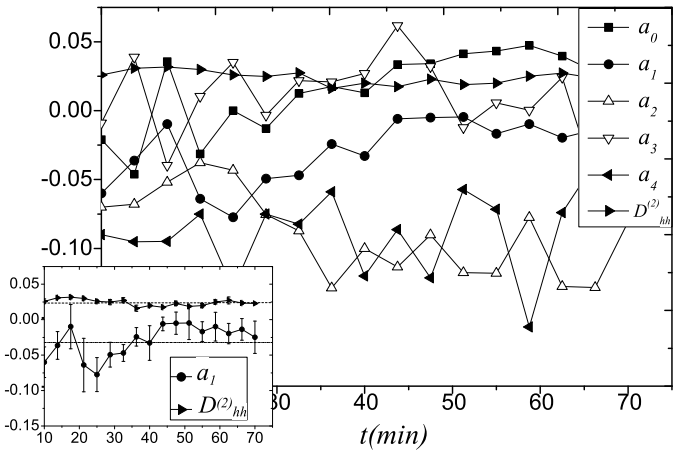

Figure 4: Dynamics of the parameters in the drift coefficients, $D_h^{(1)} = a_0 + a_1\tilde{f}_r + (a_2 + a_3\tilde{f}_r + a_4\tilde{f}_r^2)\tilde{f}_h$ and $D_{hh}^{(2)}$ components of the diffusion matrix for subject 4 (80 minutes) obtained using a 30-minute window slid in 7-minute increments. The average values of a_1 and $D_{hh}^{(2)}$ (inset) are equal to -0.032 and 0.025, respectively. They are clearly close to the values of Table 1, which were obtained by analysis of the full data set.

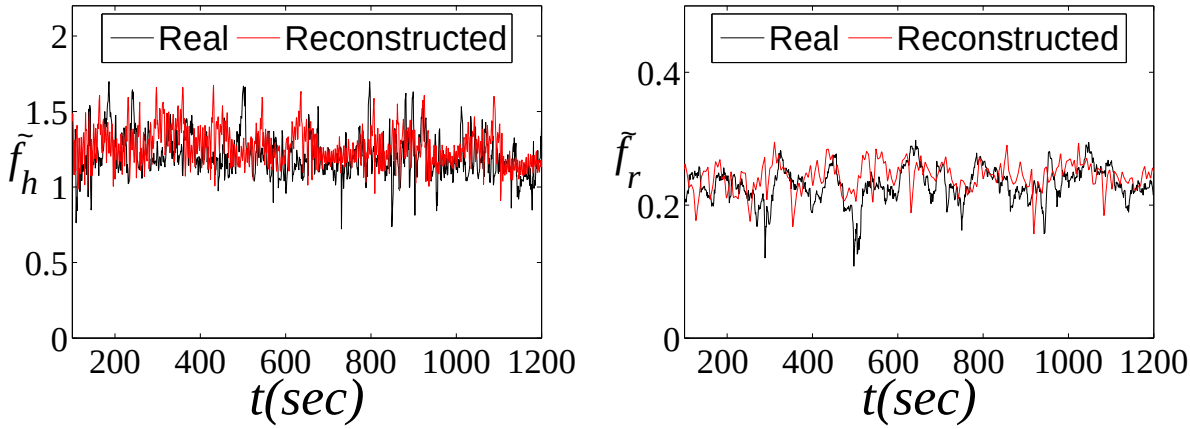

Figure 5: Comparison of the actual and reconstructed signals for $\tilde{f}_h$ and $\tilde{f}_r$.

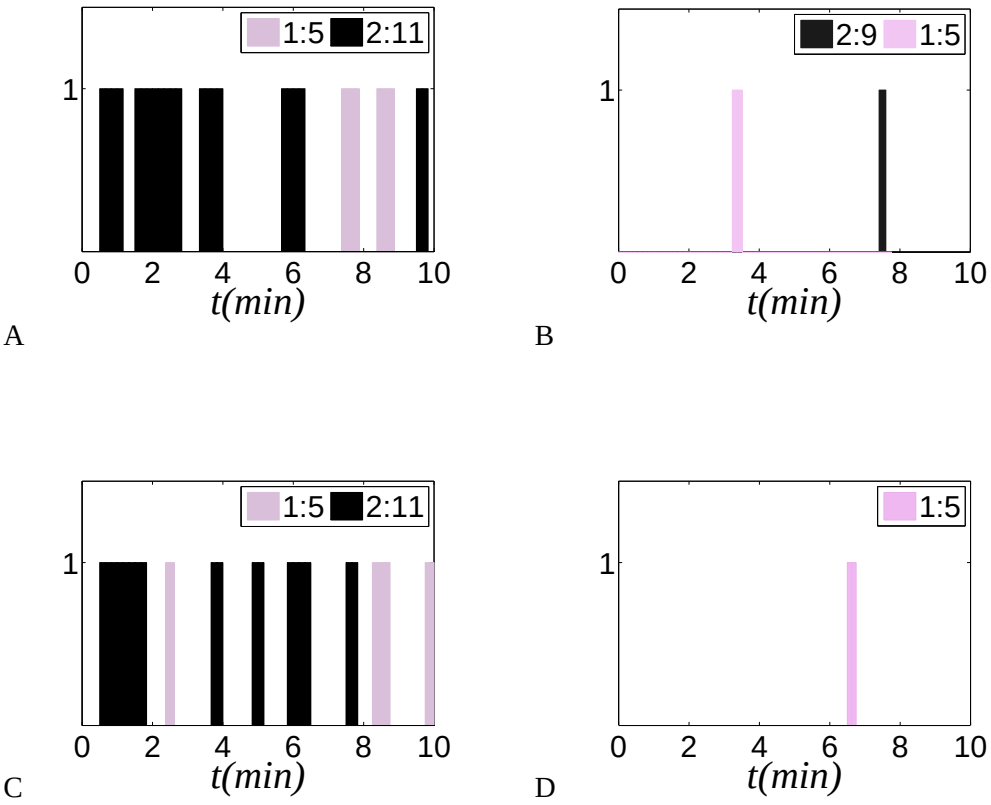

Figure 6: Episodes of synchronization derived: A from the original signals; B after shuffling of the original signals; C from the reconstructed signals; and D after shuffling of the reconstructed signals. It is evident from B and D that, even after shuffling, short epochs above threshold still occurred, albeit for durations of no more than $\sim$25 seconds. Hence, when analyzing the original data, only those epochs that exceeded 25 seconds were considered as indicative of true synchronization.